

Preparation, Characterization, and Second-Harmonic Generation of a Langmuir–Blodgett Film Based on a Rare-Earth Coordination Compound

K. Z. Wang, C. H. Huang,* and G. X. Xu

State Key Laboratory of Rare Earth Materials Chemistry and Applications, Peking University, Beijing 100871, China

Y. Xu, Y. Q. Liu, and D. B. Zhu

Institute of Chemistry, Academia Sinica, Beijing 100080, China

X. S. Zhao, X. M. Xie, and N. Z. Wu

Chemistry Department, Peking University, Beijing 100871, China

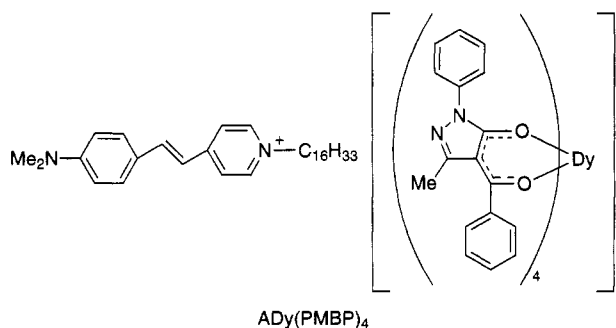
Received January 3, 1994. Revised Manuscript Received August 30, 1994[⊗]

The rare-earth coordination compound (*E*)-*N*-hexadecyl-4-(2-(4-(dimethylamino)phenyl)ethenyl)pyridinium tetrakis(1-phenyl-3-methyl-4-benzoyl-5-pyrazolonato)dysprosium(III) was synthesized. The LB films were prepared and characterized by UV–vis, IR, X-ray photoelectron spectroscopy, and low-angle X-ray diffraction. High-quality LB films up to 50 layers on the hydrophilic substrates of quartz, calcium fluoride, and glass were obtained. From the second-harmonic generation measurement, second-order molecular hyperpolarizability β of the dysprosium complex was estimated to be about $(6.6\text{--}9.3) \times 10^{-28}$ esu.

Introduction

The Langmuir–Blodgett technique is a powerful tool of forming the noncentrosymmetric structure required to exhibit second-order optical nonlinearity.¹ In addition, the LB film has a controlled thickness at the molecular level by varying not only the number of layers but also number of $-\text{CH}_2$ groups forming the hydrophobic tail so that the index of refraction can be changed simultaneously.² These features qualify the nonlinear LB films for various potential applications in various areas of optoelectronics including optical communication, electrooptical device, and laser scanning.³ Among the reported nonlinear materials, the hemicyanines have high second-order molecular hyperpolarizability. However, the film-forming properties became poor as the number of layers was increased.^{4,5} Although the addition of auxiliary materials such as arachidic acid can improve the film-forming property, phase separation and instability may appear.⁶ Here, the use of a rare-earth coordination anion as both counterion and spacer may not only improve the film-forming property but also result in the ordered charge separation of the hemicyanine chromophores without the danger of the phase separation, and as a result, inferior J aggregation would

be greatly reduced. Another approach is to explore a route to prepare a high-quality LB film with an organic–inorganic superlattice, as done here to create ordered magnetic dysprosium(III) array in LB film. To our knowledge, few LB films based on the rare-earth complexes have been reported.⁷ In this publication, the preparation, characterization and second-harmonic generation for the LB films of a following rare-earth complex are reported:



Experimental Section

Materials. (*E*)-*N*-Hexadecyl-4-(2-(4-(dimethylamino)phenyl)ethenyl)pyridinium bromide and iodide were prepared according to the literature.⁸ Rare-earth metal complex (*E*)-*N*-hexadecyl-4-(2-(4-(dimethylamino)phenyl)ethenyl)pyridinium tetrakis(1-phenyl-3-methyl-4-benzoyl-5-pyrazolonato)dysprosium(III) (ADy(PMBP)₄) was prepared according to the modified method of literature.⁹ The details of synthesis and characterization will be published elsewhere.

* To whom correspondence should be addressed.

[⊗] Abstract published in *Advance ACS Abstracts*, October 1, 1994.

(1) Neat, D. B.; Petty, M. C.; Roberts, G. G.; Ahmad, M. M.; Feast, W. J. *J. Electron. Lett.* **1986**, *22*, 460.

(2) Lupo, D.; Prass, W.; Scheunemann, U.; Laschewsky, A.; Ringsdorf, H. *J. Opt. Soc. Am. B* **1988**, *5*, 300.

(3) Williams, D. J. *Angew Chem., Int. Ed. Engl.* **1984**, *23*, 690.

(4) Girling, I. R.; Cade, N. A.; Kotinsky, P. A. *J. Phys. D: Appl. Phys.* **1986**, *19*, 2065.

(5) Li, Y. L.; Zheng, J. B.; Wang, W. C.; Zhang, Z. *Opt. Commun.* **1992**, *93*, 207.

(6) Neal, D. B.; Petty, M. C.; Roberts, G. G.; Ahmad, M. M.; Feast, W. J.; Girling, I. R.; Cade, N. A.; Kotinsky, P. V.; Peterson, I. R. *J. Opt. Soc. Am. B* **1987**, *4*, 950.

(7) Huang, C. H.; Wang, K. Z.; Gan, L. B.; Xu, G. X. *Prog. Nat. Sci.* **1993**, *3*, 306.

(8) Girling, I. R.; Cade, N. A.; Kotinsky, P. N.; Earls, J. D.; Cross, G. H.; Peterson, I. R. *Thin Solid Films* **1985**, *132*, 101.

(9) Huang, C. H.; Zhu, X. Y.; Wang, K. Z.; Xu, G. X. *Chin. Chem. Lett.* **1991**, *2*, 741.

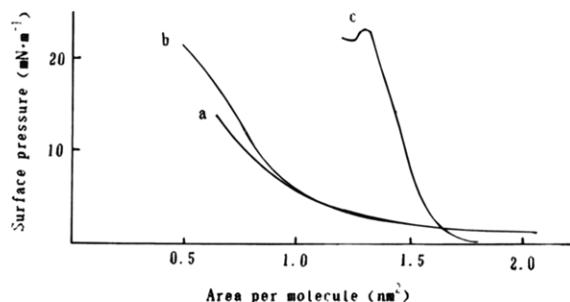


Figure 1. Surface pressure–area isotherms: (a) $\text{Me}_2\text{NC}_6\text{H}_4\text{-CH=CHC}_5\text{H}_4\text{NC}_{16}\text{H}_{33}\text{Br}$; (b) $\text{Me}_2\text{NC}_6\text{H}_4\text{CH=CHC}_5\text{H}_4\text{NC}_{16}\text{H}_{33}\text{I}$; (c) the dysprosium complex.

LB Film Preparation. The film preparations were carried out on a KSV 5000 fully computer-controlled Langmuir trough. The monolayers of the compounds were formed by dropping their benzene solution ($(0.668\text{--}4.69) \times 10^{-3}$ mol/L) onto a pure water subphase (18°C , pH 5.6). After the vaporization of the solvent, surface pressure–area ($\pi\text{-A}$) isotherms were recorded at a compression rate of 15 mm/min. The films were deposited on up- and down-stroke (Z- or Y-type) onto hydrophilically pretreated substrates with a deposit rate of 5 mm/min at a constant surface pressure of 12 mN/m. The substrates were hydrophilicity treated as before.⁹

Optical Characterization. The UV–vis spectra of the LB films on quartz substrates and dysprosium complex in chloroform were taken on a Shimadzu UV-240 spectrophotometer, using blank quartz and the solvent as references. IR spectra were measured on a Nicolet 7199B FT-IR spectrometer. X-ray photoelectron spectra were taken on ESCA LAB-5 system at a constant pass energy of 20 eV. The excitation source were Al $K\alpha$ radiation with an energy of 1486 eV, the chamber pressure was 8×10^{-6} mbar. For calibration purpose, C(1s) line was set at 286.4 eV as standard. X-ray diffractograms were obtained on a Rigaku D/max-3B diffractometer, Cu $K\alpha$ radiation with a wavelength of 0.154 nm was used.

Second Harmonic Generation (SHG). SHG from the monolayers were measured in the transmission geometry using 1.06 μm output from a Q-switched Nd:YAG laser. A $1/4$ λ plate and a Glan-Taylor polarizer were used to vary the polarization direction of the laser beam. The linearly polarized laser light was directed at 45° angle of incidence onto the vertically mounted sample. A set of 1.06 μm filters and a monochromator were used to ensure that only second harmonic radiation was detected. The second harmonic signals were detected by a photomultiplier. The average output signals were recorded on a figured storage recorder (HP54510A).

Results and Discussion

Monolayers at the Air–Water Interface. Surface pressure–area ($\pi\text{-A}$) isotherms for hemicyanines containing bromide, iodide, and the dysprosium complex anion are shown in Figure 1. The condensed region slope of the dysprosium complex is 0.76, while those for bromide and iodide are only 0.3 and 0.4. Therefore the film-forming property is apparently improved as bromide and iodide ions were replaced by the metal complex anion. The increase in film modules is most likely due to the regularity of morphology shown in Figure 2. The limiting area of $1.60\text{ nm}^2/\text{molecule}$, obtained from extrapolation of the condensed region of the complex to $\pi \rightarrow 0$, is much larger than the calculated area ($1.05\text{ nm}^2/\text{molecule}$)⁹ of the dysprosium complex anion, showing that packing within the monolayer is controlled by both the hemicyanine cation and the complex anion, they are packed together “shoulder” to “shoulder”. The experimental molecular area 1.08 nm^2

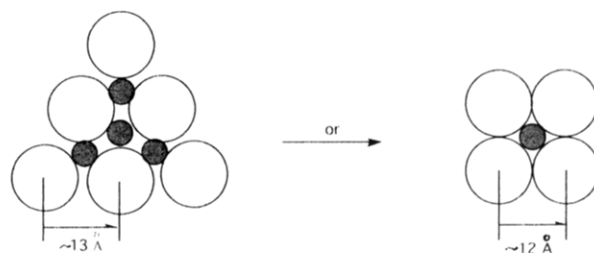


Figure 2. Possible packing arrangement of the dysprosium complex within the LB film: (●) hemicyanine cation; (○) the dysprosium complex anion.

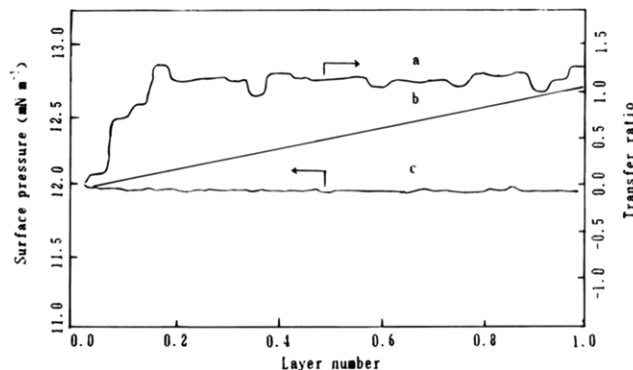


Figure 3. Monitored film-forming parameters during the film deposition: (a) transfer ratio, (b) mean transfer ratio, and (c) surface pressure.

of the hemicyanine iodide is much larger than expectation. This is due to slight water solubility of the hemicyanine.¹² But, the dysprosium complex is scarcely soluble in the pure water subphase, and this is supported by analysis.

Film Deposition Behavior. The LB films of the dysprosium complex were capable of being deposited onto fused quartz, single-crystal CaF_2 , and glass up to 50 layers. The monitored dynamic transfer of the film (curve a), transfer ratio (curve b), and surface pressure (curve c) during the film deposition on quartz substrate are shown in Figure 3, reflecting the excellent film transfer with a mean transfer ratio of 1.087 and a constant surface pressure of 12 mN/m. In addition, the transfer ratio still remain around unity as the number of layers increased up to at least 50. On the contrary, the film transfer of hemicyanine bromide or iodine became difficult, as the number of layers deposited was increased.

UV–vis Spectra. UV–vis absorption spectra for the ligand HPMBP, hemicyanine bromide, and the metal complex in CHCl_3 , as well as the LB film of the metal complex on both sides of quartz are depicted in Figure 4, respectively. It can be seen that the LB film of the metal complex exhibits a peak at 496 nm, usually assigned to the $\pi \rightarrow \pi^*$ charge-transfer transition of hemicyanine chromophore, but this peak is split in the LB films of the dysprosium complex, showing the coexistence of two kinds of species, namely, the monomeric and aggregated, and that the complex anion can take on a role of separating the chromophore of the hemicyanine-like fatty acid. However, here the complex anion acts as both counterion and spacer; this has no potential disadvantage of the phase separation, which was verified by the low-angle X-ray diffraction discussed latter. The UV spectrum for the dysprosium complex in chloroform resembles that for the LB film. They both

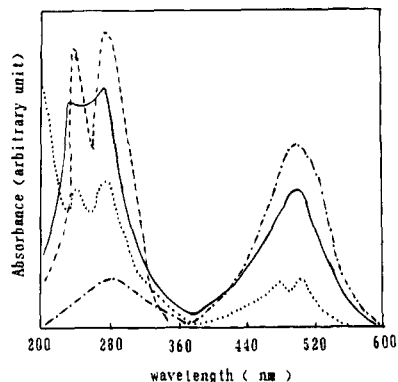


Figure 4. UV-vis spectra: (---) HPMBP in CHCl_3 ; (—) the dysprosium complex in CHCl_3 ; (···) five layers of the LB film for the dysprosium complex; (- · - ·) $\text{Me}_2\text{NC}_6\text{H}_4\text{CH}=\text{CH}-\text{C}_5\text{H}_4\text{NC}_{16}\text{H}_{33}\text{Br}$ in CHCl_3 .

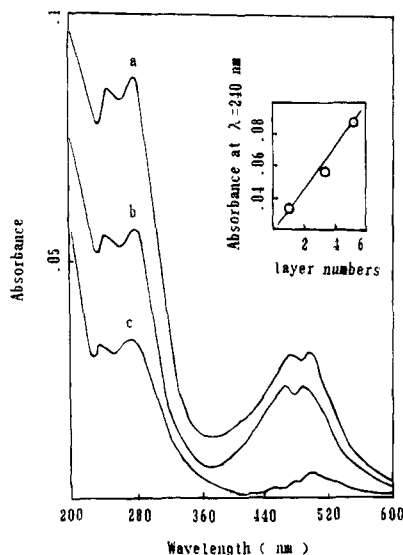


Figure 5. UV-vis spectra of the LB films of different number of layers. Curve (number of layers): a (5); b (3); c (1).

have similar two peaks at ca. 240 and 280 nm, which is the characteristic absorption of HPMBP, showing that the weak UV absorption of the hemicyanine cation is obscured by the strong absorption of HPMBP. The peak at 248 nm of free HPMBP undergoes a small blue-shift of 8 nm upon ligation, which is usually assigned to $n \rightarrow \pi^*$ electronic transition on carbonyl group, while the peak at 280 nm which corresponds to the $\pi \rightarrow \pi^*$ electronic transition on the benzene ring in HPMBP remains unchanged. The absorbance at a wavelength of 240 nm was measured as a function of the number of layers deposited and was found to be linearly dependent on the number of layers (inset in Figure 5), showing that the film is vertically uniform.

IR Spectra. The IR spectrum for the powder metal complex is very similar to that for the 50-layer LB film on CaF_2 substrate. The HPMBP peaks at 1646 and 1600 cm^{-1} for $\nu_{\text{C}=\text{O}}$, $\Delta\nu = 46 \text{ cm}^{-1}$. For the powder complex, the former blue-shifts to 1579 cm^{-1} , the latter red-shifts to 1615 cm^{-1} , $\Delta\nu = 36 \text{ cm}^{-1}$. For the LB film, to 1579 and 1612 cm^{-1} , $\Delta\nu = 33 \text{ cm}^{-1}$. The former is usually assigned to the vibration of carbonyl group on the pyrazolone ring; the latter to that of 4-positional benzoyl. The bond length of $\text{C}=\text{O}$ tend to be unified upon ligation, resulting in the reduction of $\Delta\nu$. Also, the weak and broad $\nu_{\text{OH}-\text{O}}$ peak between 2600 and 3000

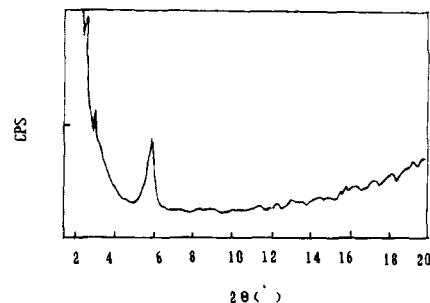


Figure 6. Low-angle X-ray diffractogram for 48 layers of LB film on glass plate.

cm^{-1} for HPMBP disappears in the spectra of the powder complex and the LB film. This is also indicative of the coordination of oxygen in the carbonyl of HPMBP and no occurrence of free HPMBP. Therefore, it can be concluded that the film was formed by the target metal complex and that it could be deposited safely without side reaction such as the hydrolysis of metal ion, but the hydrolysis of metal ion happened in the LB films of rare-earth stearate.¹⁰

X-ray Photoelectron Spectra. X-ray photoelectron spectra for both the powder metal complex and the 50-layer LB film on glass substrate appears the characteristic peaks with the binding energy of ca. 1297 eV for $\text{Dy}3d_{5/2}$, 156 eV for $\text{Dy}4d_{5/2}$, 531.4 eV for O1s, 400 eV for N1s, and 284.8 eV for C1s, respectively. Atom number ratio C:O:N of 10:1.2:1 for the LB film and 10.1:0.89:1 for the powder complex were obtained. The latter is consistent with the theoretical value (9.9:0.8:1), but the former give an oxygen content larger than expected, the excessive oxygen originating from the glass substrate. Peak intensity ratio of Dy3d to C1s from the powder complex divided by that from the LB film is found to be 1.12, which is considered to be caused by varied Dy depth distribution resulted from the organized lamellar structure of LB film.¹¹

Low-Angle X-ray Diffraction. Low-angle X-ray diffractogram for the 48-layer LB film on glass plate is shown in Figure 6. A well-defined film structure is revealed by contrasting regular diffraction characteristics from the LB film with that from polycrystalline pattern of powder complex, peaks at 2θ 1.5, 2.96, and 6.08° are assigned to (001), (002), and (004) Bragg diffraction, respectively, and average layer spacing 58.8 Å was obtained according to Bragg equation. The single-layer film thickness 29.4 Å was thus derived based on the Y-type structure of the film. The film on CaF_2 plate 113 days after deposition exhibits similar peaks at 2θ 3.08, 6.14, and 21.4° assigned to (002), and (008) diffraction, respectively, and the film thickness 28.7 Å was similarly calculated. This shows that the film have good time stability.

Second Harmonic Generation. On the assumption that the hemicyanine chromophores have a common tilt angle, ϕ , with a random azimuthal distribution and that second-order molecular hyperpolarizability (β) is dominated by the component along the intramolecular donor- π -acceptor axis, the following equations can be

(10) Yang, K. Z.; Xiao, T.; Mu, J. *Acta Chim. Sin. (China)* **1991**, *49*, 340.

(11) Chen, H. J.; Chai, X. D.; Wei, Q.; Li, T. J. *Chem. J. Chin. Univ. (China)* **1991**, *12*, 524.

obtained:¹²

$$\frac{I_{2\omega}(\mathbf{p}\rightarrow\mathbf{p})}{I_{2\omega}(\mathbf{s}\rightarrow\mathbf{p})} = \frac{(\chi_{zzz}^{(2)} \sin^3 \theta + 3 \chi_{zxx}^{(2)} \sin \theta \cos^2 \theta)^2}{(\chi_{zxx}^{(2)} \sin \theta)^2} \quad (1)$$

$$\chi_{zzz}^{(2)} = \chi^{(2)} \cos^3 \phi = N f_{2\omega} (f_{\omega})^2 \beta \cos^3 \phi \quad (2)$$

$$\chi_{zxx}^{(2)} = 0.5 \chi^{(2)} \cos \phi \sin^2 \phi = 0.5 N f_{2\omega} (f_{\omega})^2 \beta \cos \phi \sin^2 \phi \quad (3)$$

in which $\theta = 45^\circ$ is the angle of the laser beam to the film. In the SHG experiment, the polarization-dependent double-frequency signal intensity $I_{2\omega}(\mathbf{p}\rightarrow\mathbf{p}) \gg I_{2\omega}(\mathbf{s}\rightarrow\mathbf{p})$, with $I_{2\omega}(\mathbf{p}\rightarrow\mathbf{s}) \sim I_{2\omega}(\mathbf{s}\rightarrow\mathbf{s}) \sim 0$. The ratio of the intensities and the combination of eqs 1–3 can obtain the tilt angle ϕ with respect to the surface normal of the film; N is the number of molecules per unit volume; $f_{\omega,2\omega} = [(n_{\omega,2\omega}^2 + 2)/3]$ is a local field correction factor, where n_{ω} and $n_{2\omega}$ are the refractive indexes of the film at fundamental and second harmonic frequencies, respectively, and the $n_{2\omega}$ is usually slightly higher than the n_{ω} ,^{2,13} but in this treatment, n is taken to be $n_{\omega} \approx n_{2\omega} = 1.7$.¹² From comparison of the SH signals with that from quartz reference (d_{11} , 0.5 pm V^{-1}), the susceptibility $\chi^{(2)}$, second-order molecular hyperpolarizability β were obtained based on eqs 2 and 3. These values are shown in Table 1.

It can be seen from Table 1 that the tilt angle ϕ is largely decreased as the bromide or iodide counter ion is replaced by the dysprosium complex anion. It is also noteworthy that the β value of the dysprosium complex is about 2 times larger than that of hemicyanine iodide. It was reported that the 1:1 film of the hemicyanine and

Table 1. Comparison of SHG from Monolayer Films^a

compounds	$\chi^{(2)} \times 10^6$ (esu)	$\beta \times 10^{28}$ (esu)	ϕ (deg)	ref
AI	0.35–0.50	2.4–3.6	40	this work
ADy(PMBP) ₄	0.59–0.87	6.6–9.3	29.1	this work
BI	0.55–0.85	1.7–2.7	41	12

^a A = $(\text{CH}_3)_2\text{NC}_6\text{H}_4\text{CH}=\text{CHC}_5\text{H}_4\text{NC}_{16}\text{H}_{33}^+$. B = $(\text{CH}_3)_2\text{NC}_6\text{H}_4\text{CH}=\text{CHC}_5\text{H}_4\text{NC}_{18}\text{H}_{37}^+$.

behenic acid exhibits a large bathochromic shift of the absorption band from 439 to 477 nm and 44-fold increase in SH intensity.¹⁴ This is due in part to resonant enhancement. However, the dysprosium complex has nearly the same spectral overlap at the harmonic wavelength as the hemicyanine iodide. As a result, the enhanced SH signals are not responsible for the resonant enhancement and most likely be attributed to the ordered separation of hemicyanine chromophores by the bulky dysprosium complex anion.

Conclusion

In conclusion, we prepared the high-quality LB film of a rare-earth complex with large second-order molecular hyperpolarizability β ; this is most likely due to the use of a bulky rare-earth anion which forces charge separation and allows more charge delocalization in the hemicyanine chromophore. This greatly enhances β and affects the spectral characteristics observed. Regular X-ray diffraction patterns reflecting the ordered structure of the film were obtained even 113 days after deposition. In the meantime, magnetic rare-earth ion was introduced into the film. Studies on related properties are under way.

Acknowledgment. This project was supported by The Climbing Program, a National Fundamental Research Key Project, and NNSFC.

(12) Ashwell, G. J.; Hargreaves, R. C.; Baldwin, C. E.; Bhara, G. S.; Brown, C. R. *Nature* **1992**, *357*, 395.

(13) Shen, Y. Q.; Shen, J. F.; Chiu, L.; Zhu, Z. Y.; Fu, X. F.; Xu, Y.; Liu, Y. Q.; Zhu, D. B.; Wang, W. C.; Liu, L. Y. *Thin Solid Films* **1992**, *208*, 280.

(14) Schildkraut, J. S.; Penner, T. L.; Willand, C. S.; Ulman, A. *Opt. Lett.* **1988**, *13*, 133.